International Journal of Modern Manufacturing Technologies
ISSN 2067–3604, Vol. XIV, No. 2 / 2022
https://doi.org/ 10.54684/ijmmt.2022.14.2.272

NUMERICAL INVESTIGATIONS ON THE FREE SURFACE FLOW AROUND WING-BODY JUNCTIONS

Costel Ungureanu[1], Claudia-Veronica Ungureanu[2]

[1]Department of Naval Architecture, Faculty of Naval Architecture, "Dunarea de Jos" University of Galati, 47 Domneasca Street, 800008, Galati, Romania
[2]Department of Applied Sciences, Cross-Border Faculty, "Dunarea de Jos" University of Galati, 47 Domneasca Street, 800008, Galati, Romania

Corresponding author: Costel Ungureanu, costel.ungureanu@ugal.ro

Abstract: Starting with January 2013, all ships greater than 400 tons engaged in international voyages must comply with the Energy Efficiency Design Index (EEDI), and starting with January 2023 also with the Efficiency Existing Ship Index (EEXI), issued by the International Maritime Organization, (IMO). Knowing that, in general, a ship hull is the result of a compromise between the main dimensions imposed by the size of the locks, navigation route depth, port depth, taxes, transport capacity (deadweight, volume), ship equipment (machinery, deck installations, piping systems), hydrostatic performances and last but not least the hydrodynamic performances, from ship hydrodynamics point of view the available approaches are the optimization of the ship size and hull forms or the design of propellers adapted to the ship's wake. The main purpose is to reduce the ship resistance and increase the efficiency of the propulsion system which ultimately leads to a reduction in the power placed on board the ship. For this, there can be used the so-called flow control devices or Energy Saving Devices (ESD hereafter), as hydrofoils or nozzles, to improve the flow parameters entering the propeller disc in order to increase the efficiency of the propulsion system and decreasing the fuel consumption leading to reducing of the carbon and greenhouse gasses emissions. For ballast loading condition the ESD may intersect the free surface, the flow becoming complicated and combining nonlinear, three-dimensional and turbulent phenomena such as the boundary layer on solid surfaces, the horseshoe vortex system developed around junctions and their effects turbulence, and also wave breaking. Therefore, this paper presents the results of the numerical study on the viscous free surface flow around junctions between a hydrofoil mounted on a plate, more precisely the study of the influence of the angle between hydrofoil and plate. It was observed that from a hydrodynamic point of view the angle between hydrofoil and base plate to be less than 15 degrees in respect to the vertical direction on the hydrofoil so that horseshoe vortex to be reduced in intensity and the value of the hydrofoil drag to be minimal.

Key words: numerical investigation, surface-flow, wing-body

1. INTRODUCTION

In recent years, interest in global warming has grown significantly, and topics such as energy efficiency, environmental pollution, and the reduction of greenhouse gas emissions are a hot topic. International efforts to reduce the impact of climate change began in 1992 in Rio, where more than 150 governments signed a framework agreement for sustainable development. The Kyoto Protocol [1] was adopted in 1997, by which the signatory states, 37 industrialized states and the European Community, committed themselves to reducing the level of greenhouse gases by an average of 5.2% by 2012 compared to 1990. Internationally, shipping has not been explicitly addressed in the Kyoto Protocol, Annex 1. Instead, public and political agenda on greenhouse gas emissions from shipping has shifted to the International Maritime Organization (IMO). According to the [2], "the most comprehensive and authoritative estimate of greenhouse gases in the naval field", in 2007, the shipping of goods produced approximately 1046 million tons of gas emissions, representing approx. 3.3% of global emissions, of which 870 million tons of carbon dioxide (CO2), 2.7% globally. Carrying out calculations on various emission scenarios, the IMO has found that in the absence of concrete environmental policies, by 2050, CO_2 emissions will increase by 150-200% compared to 2007, so that from 1 January In 2013, the Energy Efficiency Design Index (EEDI) and the Energy Efficiency Operational Indicator (EEOI) became mandatory for all ships over 400 tonnes, [3]. According to the IMO resolution, these indices are specific to each type of ship and should be reduced by 2025 by up to 30% from a reference value. In June 2021, IMO's Marine Environment Protection Committee [4], adopted amendments to the International Convention for the Prevention of Pollution from Ships (MARPOL) Annex VI that will

require ships to reduce their greenhouse gas emissions. These amendments, mandatory with 1st of January 2023, combine technical and operational approaches to improve the energy efficiency of ships, also providing important building blocks for future GHG reduction measures. The new measures will require all ships to calculate their Energy Efficiency Existing Ship Index (EEXI) following technical means to improve their energy efficiency and to establish their annual operational carbon intensity indicator (CII) and CII rating. Carbon intensity links the GHG emissions to the amount of cargo carried over distance travelled. In fact, these indices represent the ratio between the total CO_2 emissions on board the ship and the transport capacity, speed and parameters related to the ship's operating conditions. Also, the Ukraine crisis has led to a decline in maritime exports of raw materials (ore, grain, crude oil) from Ukraine and Russia to the rest of the world. To meet the need for raw materials, companies have shifted to other markets. As a result, the need for high-capacity cargo ships (bulk carriers, miners, oil tankers) has increased. These ships are equipped with slow, two-stroke engines that run on heavy fuel oil, with high greenhouse gas emissions. In this context in which, from 1 January 2023, ships must demonstrate significant reductions in greenhouse gases, these appendices becomes a very good solution, especially been suitable for ships already in operation for which the EEXI index is to be applied. In the case of ships in service, it is no longer possible to intervene on the outer shell to change the hull, but only for local repairs, and such devices can be welded to ship's hull with minimal costs at the first docking of the ship.

These so-called flow control devices or ESD, are in general hydrofoils, nozzles or combination of both, and their main purpose is to improve the flow parameters entering the propeller disc in order to increase the efficiency of the propulsion system and decreasing the fuel consumption leading to reducing of the carbon and greenhouse gasses emissions. For ballast loading condition the ESD may intersect the free surface, the flow becoming complicated and combining nonlinear, three-dimensional and turbulent phenomena such as the boundary layer on solid surfaces, the horseshoe vortex system developed around junctions and their effects turbulence, and also wave breaking, for both types nozzles or hydrofoils, either solitaire or multiple. A detailed description of the flow control devices was presented by [5].

A detailed procedure for design of marine screw propellers in combination with stators is described by [6], also known as fixed guide vanes or pre/post swirl devices, based on lifting line theory involving the realistic representation of the propeller slipstream, which is contracted form of helical vortices.

The flow with and without free surface flow around the juncture between a plate and a symmetrical hydrofoil has been presented by [7, 8] considering different inclination angle of the foil. The first study was concentrated on completely submerged junction with a profile inclined in 3 directions with three angle steps, s, mounted on a flat, concave or convex base plate (at 4 radii of curvature), at three Reynolds numbers, 10^6, $5x10^6$ and 10^7. The second paper is studying the interaction between free surface flow and junction flow for a hydrofoil mounted on a flat plate.

A study on the effects of a nozzle placed in front a propeller was presented by [9], and through systematically conducted simulations observed that the net thrust reflecting the overall drag, which includes the nozzle, depends on the duct size. The duct presence determines two regions of the inflow into the propeller. One is the inner region of the nozzle where the high-speed flow exists because of the contraction of the duct. The other is the outer region of the nozzle where the flow decelerates due to the duct wake. Lower- and higher-pressure coefficients on the suction and pressure sides, cover a significantly wider area than those of the case without the nozzle, leading therefore to greater thrust and torque. The existence of a critical attack angle for which the magnitude of the relative axial force becomes maximum for the smallest nozzle diameter has been noticed.

The authors of paper [10] introduced a combined solution between fins and nozzle with an improved fuel efficiency up to 10%. This system creates optimal inflow for the propeller by guiding one side of the stern flow in the opposite direction to the propeller's direction of rotation, generating pre-swirl. The solution consists of multiple curved fins interconnected by a ring and attached to the ship's hull to prevent the power losses that typically occur in a propeller's slipstream. The fins enhance the propeller's efficiency while keeping resistance at acceptable levels and the ring reduces the tip vortex while also levelling out the peak stresses that occur in severe loading conditions such as slamming.

A systematic study of appendages influence on ship resistance at model scale has been performed by [11] based on RANS-VOF simulation. Six appendages configurations at five different Froude number have been investigated. The predicted total resistance coefficient computed for hull with skeg showed a good agreement with a difference of less than 2% than experimental data Analysis of computational results revealed that the main contribution in drag, of about 8 percent, is added by the rudder and the shaft. The maximum effect of the appendages on the ship drag is 28.7 % and it appears for the Froude number 0.35.

An investigated over the ventilation elimination mechanisms during the deceleration process of a surface-piercing hydrofoil using the unsteady

Reynolds-averaged Navier-Stokes (RANS) method together with a Volume of Fluid (VOF) model I presented by [12]. The ventilation elimination mechanism of the surface-piercing hydrofoil was analysed from the perspectives of the hydrofoil hydrodynamic performance, the ventilated cavity evolution, vortex structures, and re-entrant jets.

The flow around the appendages mounted on the hull of the ship is a simple configuration but with a complicated topology and can be controlled by a judicious design of the geometries of the components, so that the regime of pressure fluctuations, induced vibrations and energy consumption can be controlled from exterior. Flow control is also of practical relevance because it can significantly influence the lift or resistance to advance, stability characteristics by controlling the topology and intensity of vortex structures or can lead to sources of noise or structural vibration. Also, the free surface flow around hydrofoils with bluff leading edge may be manifested by wave breaking and cavitation. Thus, in the global economy of the ships performances, such appendages may further contribute to the ships drag on the one hand, but at the same time may complicate the flow in the aft part of the ship leading to unevenness in the flow field in the vicinity of the propeller, another, contrary to the purpose of using these devices. As a result, this research aims to systematically study the influence of the inclination of the profile, on the support plate and the free surface over the flow topology around the junction. First, the profile mounted vertically on the flat plate will be studied. It will tilt in three steps, 15^o at a time, first in the plane perpendicular to the plane of symmetry of the profile, and then in the plane of symmetry upstream and downstream, while maintaining the leading edge parallel to the trailing edge. The chosen aero-hydrodynamic profile is a symmetrical one, intensively studied and used in aerodynamics, NACA 0012, for which there is information in the literature on the dependence of the drag on the Reynolds number as well as the distribution of pressure and friction coefficients on the profile chord.

2. NUMERICAL MODEL

Given that numerical simulations provide a quantitative prediction of simultaneous flow for all physical quantities investigated, in a very large number of points in time and space, substantially reducing design and production time and costs, and taking into account the multitude of geometric configurations of the appendages, the possibility of the influence of the free surface in the proposed research it will be used numerical simulations in the parametric calculations of the angle between the hydrofoil and the base plate.

Free surface flow around a hydrodynamic profile mounted on a plate near the free surface is a complicated one that combines nonlinear, three-dimensional and turbulent phenomena such as the boundary layer on solid surfaces, the horseshoe vortex system developed around junctions and the effects of the free surface as if turbulent, breaking the wave. Due to the complexity of the discretization grid generated on a computational domain with constraints imposed by numerical resolution of the free surface calculating method implemented in the Ansys Fluent program, numerical simulations were performed only for the junction between the hydrodynamic profile and the flat plate.

2.1. Boundary conditions

When flowing at free surface, the surface penetrating foil generates a system of divergent waves whose windings propagate at an angle of about 20°. In order to avoid the radiation of the waves upstream, the inlet boundary condition is arranged at 1.5 foil chord upstream of the leading edge. In order to avoid the reflection of the wave system from the lateral boundaries, producing numerical instabilities, the width of the calculation range as well as the length of the downstream area are established so that the wave system leaves the entire domain through the outlet boundary. As a result, the downstream boundary is arranged at five chord lengths from the profile trailing edge, and the side borders at two 2.5 chord lengths from the plane of symmetry. The position of the upper boundary is chosen so as to allow the natural elevation of the free surface (figure 1). Initial tests determined that 0.5 of the profile chord length is sufficient.

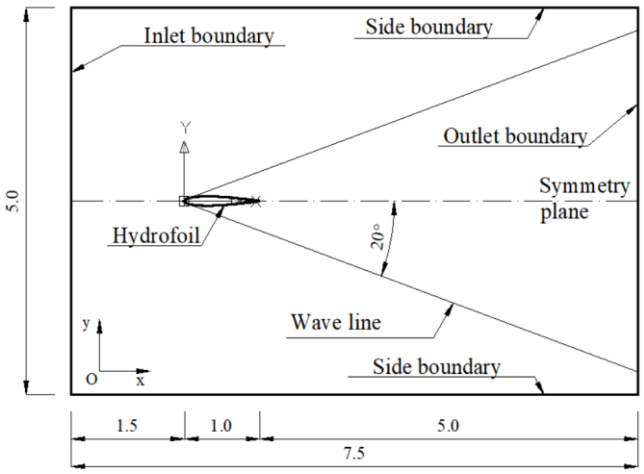

Fig. 1. Computational domain dimensions.

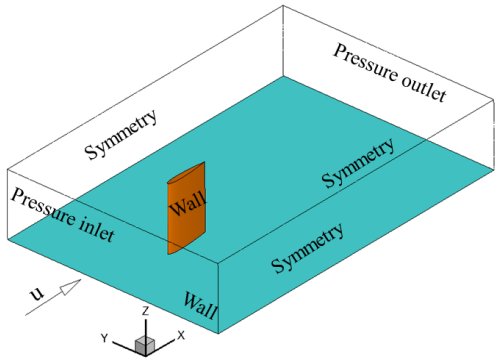

Fig. 2. Boundary conditions.

Free surface flow is governed by gravitational force and inertial forces, represented by the dimensionless parameter Froude. As a result, the boundary conditions imposed must take into account the effects of gravity. In this sense, the calculation domain is modelled for open channel flow. Figure 2 shows the computational domain together with the boundary conditions imposed. Fluid inlet and outlet boundaries in the field are defined as pressure inlet and pressure outlet. On these, the level of the initial calm free surface is declared, as well as the level of the bottom of the aquarium for the solver to calculate the hydrostatic pressure. Also, the fluid velocity at infinite upstream and the initial turbulent sizes are declared. In the case of the k-ω SST turbulence model, the turbulence intensity, calculated on the basis of the hydraulic diameter, and the ratio of turbulence to molecular viscosity shall be declared. In the problems with the free surface flow, the calculation range is defined from a single volume, following that after the initialization of the simulation, the zones for the two fluids water and air will be declared. On the strut and on the plate, the no slip condition, of the wall type, is required. The condition of symmetry shall be declared on the lateral boundaries as well as on the upper boundary of the computational domain. In the present study, the explicit, quasi-stationary calculation with advancement in time, proved to be a much more robust and stable alternative than the stationary calculation. Ansys Fluent calculation algorithm is quite robust and allows the advancement over time without distorting the results. In order not to introduce errors in the calculation, when integrating the flows on the cells, the time step necessary to integrate the flow equations is calculated based on the volume of the smallest cell in the discretization grid. The correct implementation of boundary and initial conditions is a key issue in every numerical simulation. In addition to the accuracy of the solution, the robustness and speed of convergence are fundamentally influenced by how the digital boundary mirrors the properties of the physical boundary.

2.2. Numerical schemes

To accurately simulate both hydrodynamic and aerodynamic flow, the mathematical model must capture the effects of viscous flow, the transitional nature of flow (from laminar to turbulent flow), boundary layer detachments, vortex structures, and free surface wave systems, or fluid-structure interaction. The mathematical model required for free surface flow around junctions includes: flow governance equations, turbulence modelling equations, free surface modelling equations, and equations for describing initial and boundary conditions. The RANS equation system together with the equations of the k-ω SST turbulence model are solved in a non-stationary regime, in a quasi-explicit manner, using the finite volume method from Ansys Fluent. The gradients of the solution are obtained by applying the cell-based Green-Gauss theorem. To solve hydrodynamic problems with the free surface flow, the Ansys Fluent program has implemented the VOF method. This is a surface capture technique applied to a fixed Eulerian grid, designed for two or more immiscible fluids, the free surface being the interface between the fluids. For each phase (fluid) a variable is entered: the volume fraction of each cell in the grid. In each control volume the sum of the volume fractions is equal to 1. The variables and properties in each cell are described by either a single phase or a mixture of phases. N the current study VOF method is solved using the geometric reconstruction scheme. The coupling of velocity and pressure is solved by the PISO algorithm, imposed by the non-stationary calculation. The pressure is described by the PRESTO scheme, and the convective and diffusive terms are solved by the QUICK scheme.

2.3. Grid generation

In the free surface flow calculations, the boundary conditions implemented in Fluent impose vertical boundaries for both inlet and outlet. Figure 3 shows the calculation range for the case of the profile inclined by 30 degrees in the downward symmetry plane where the delimitation lines of the component grids can be observed.

The flow around the junction is described by phenomena such as the interaction of two boundary layers, one on the plate and the other on the profile. At the same time the grid must meet quality conditions such as spacing and orthogonality on solid boundaries. In addition, if the free surface is added, the discretization for solving by the VOF method must describe a band of condensed nodes in the area where the formation of the wave system is expected.

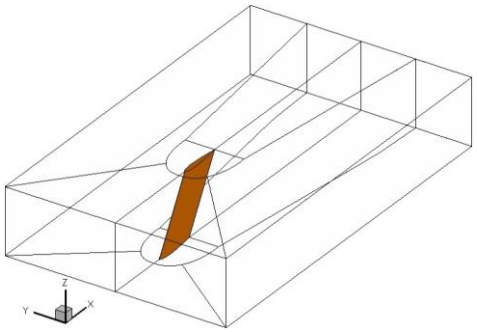

Fig. 3. Multi block calculation model, example for hydrofoil inclined with 30 degrees, downstream.

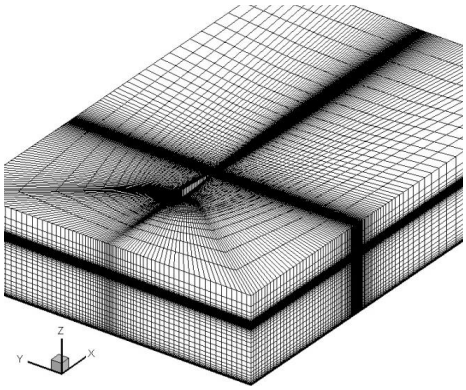

Fig. 4. C-H multi block structured numerical grid.

Taking into account all the conditions imposed for solving the imposed physical problems, a structured multi block grid is generated that overlaps perfectly on the rectangular computing field, which ensures orthogonal and condensed grid lines on the base plate and on the foil but which in the same time ensures the minimum space necessary to capture the elevation of the free surface. This results in a discretization grid with approximately two million hexahedral cells. Figure 4 shows the discretized computational domain in structured multi block style of type C-H.

3. RESULTS AND DISCUSSIONS

The influence of the angle between the profile and the plate is studied by tilting the profile in three directions: lateral, upstream and downstream, with three steps, 15, 30 and 45 degrees, starting from the position of the upright profile, always keeping the profile cord parallel to direction of flow. Together with the case of the right vertical profile it forms the set of geometric hypostases of the profile in relation to the baseplate.

The following are the vortex structures that develop when the current lines meet the attack board of the hydrodynamic profile due to the blocking phenomenon. Figure 5 shows the system of two counter-rotating vortices, one main of higher intensity and one secondary of lower intensity located in the vicinity of the leading edge of the profile as well as the evolution in relation to the inclination of the profile in the normal direction to the vertical plane of symmetry. The influence of the base plate is observed as the profile tilts, causing the main vortex to move towards the hydrodynamic profile. Also, the translation of the vortex core as well as the increase in diameter of the main vortex can be observed by presenting the velocity vectors in the plane of symmetry (figure 6).

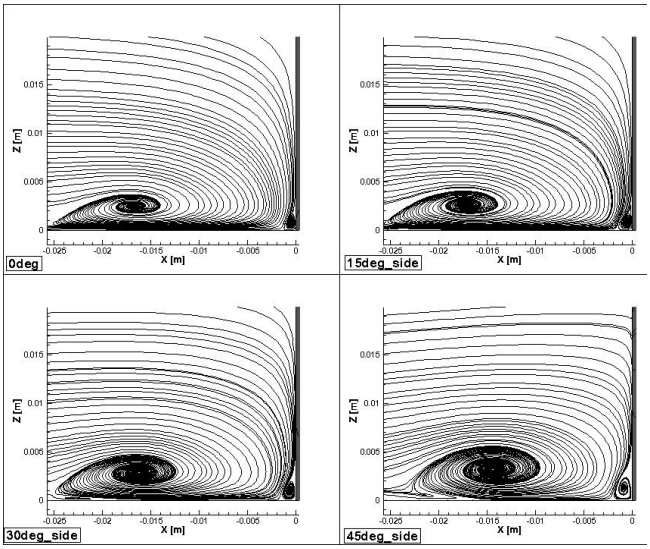

Fig. 5. Streamlines in front of leading edge, side inclination.

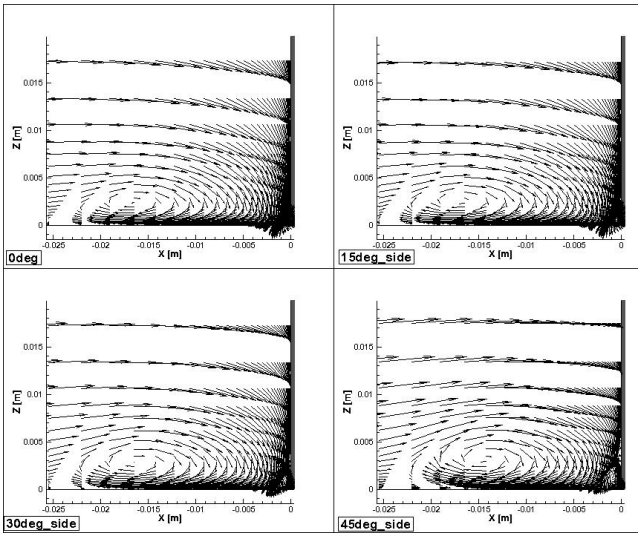

Fig. 6. Velocity vectors in front of the leading edge, side inclination.

The upstream inclined profile (figure 7) shows that the main vortex moves towards the base plate and due to the high pressure gradients generated by the presence of the two solid surfaces, at 30 and 45 degrees no more vortex structures are formed, a sustained phenomenon and of the graphical presentation of the velocity vectors in the plane of symmetry upstream of the profile (figure 8).

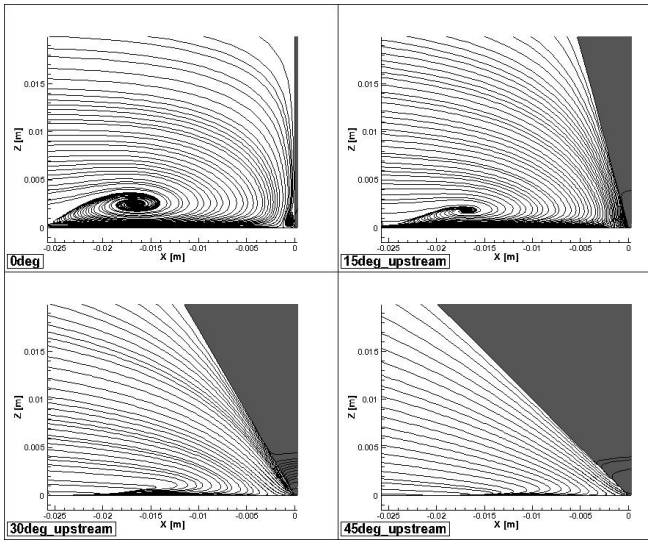

Fig. 7. Streamlines in front of leading edge, foil inclined toward upstream.

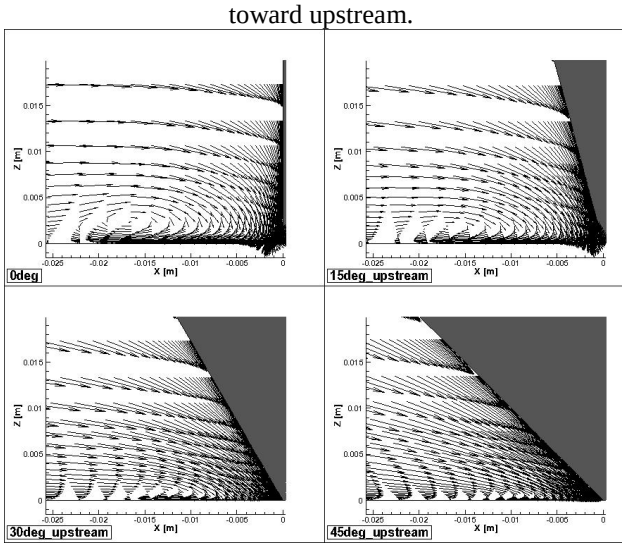

Fig. 8. Velocity vectors in front of the leading edge.

As depicted in figure 9, when the foil is inclined downstream, the streamlines approach the leading edge of the profile leading to a bypass of the position of the main vortex with the secondary one, together with the increase in intensity and diameter of the core of the main vortex. If in the upright profile case the secondary vortex is in the vicinity of the leading edge, at 30 and 45 degrees it moves away from the leading profile.

The change of position between the main vortex with the secondary vortex in relation to the increase of the downward angle of inclination can also be seen in Figure 10, in the form of velocity vectors. It can also be seen that in the upright foil profile the presence of the obstacle drives the streamlines in the downward direction, and the large angle of inclination allows the streamlines to slide in the horizontal and upward direction. This allows a reduction of the pressure gradient and thus facilitates the translation of the main vortex closer to the hydrofoil.

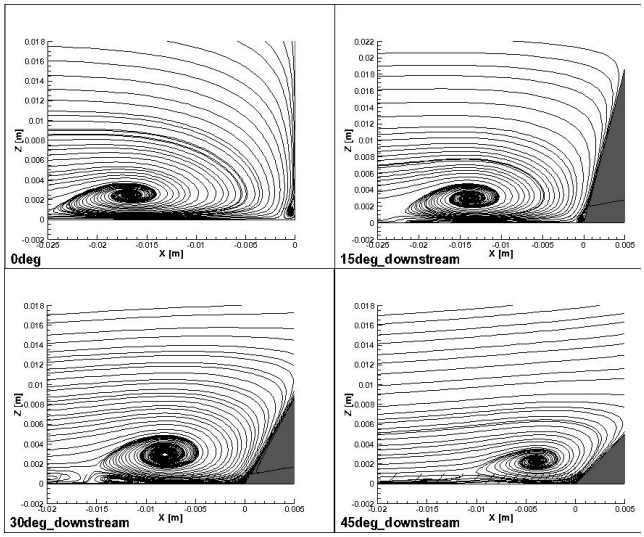

Fig. 9. Streamlines in front of leading edge, foil inclined downstream**.**

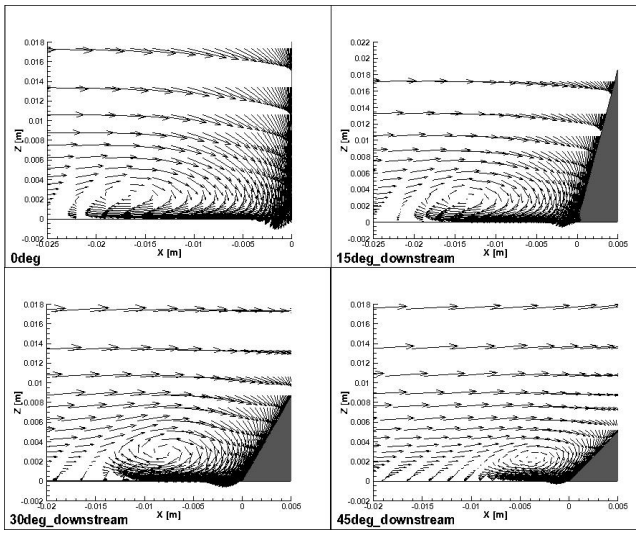

Fig. 10. Velocity vectors in front of the leading edge, foil inclined downstream.

Figure 11 and 12 show the evolution of the free surface in relation to the angle of inclination of the profile to the side. It is observed that the geometric asymmetry induces differences between the two edges of the profile and the generated wave system, asymmetry in the flow field, but also a phase shift of the ridge / wave gap alternation. The yellow and red colours show the wave crests and the shades of blue show the wave gap. There is also an increase in the size of the wave crest as well as a deepening of the wave gap as the angle of inclination increases. The numerical free surface was generated as the iso-surface of the water-air volume fraction equal to 0.5.

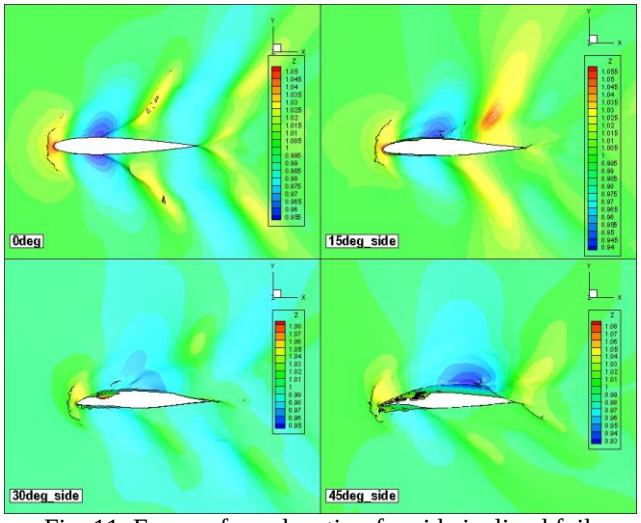

Fig. 11. Free surface elevation for side inclined foil.

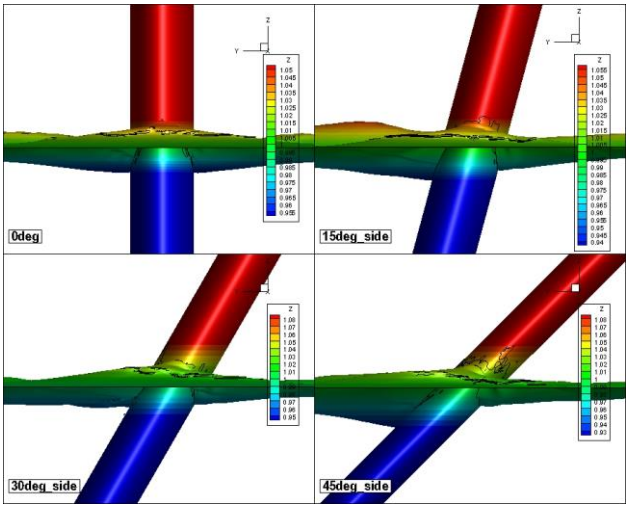

Fig. 12. Free surface elevation on surface piercing hydrofoil.

Figure 13 shows the evolution of the free surface in relation to the angle of inclination of the downstream profile. It is observed that as the angle of inclination increases, the amplitude of the first wave generated by the profile increases.

Figure 14 shows the evolution of the free surface in relation to the angle of inclination of the upstream profile. It is observed that the amplitude of the first wave generated by the profile decreases with increasing angle of inclination, because the current lines are driven downwards, similar to the junction at the base of the profile. If in the case of the straight vertical profile the second wave ridge is prominent, it decreases in amplitude as the angle between the plate and the profile increases.

Figure 15 as well as table 1 shows the drag coefficients together with the relative error in respect to the upright profile. There is a decrease of up to 10% of the total coefficient in the case of lateral inclination and a decrease of up to 55% in the case of inclination in the diametrical plane upstream and downstream.

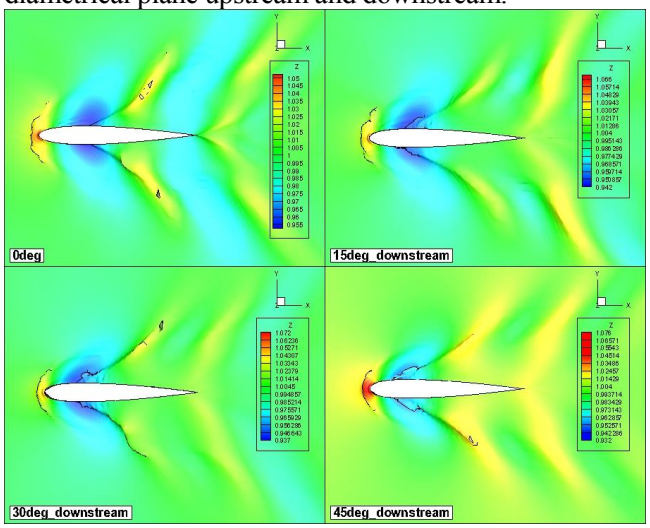

Fig. 13. Free surface elevation for side inclined toward downstream

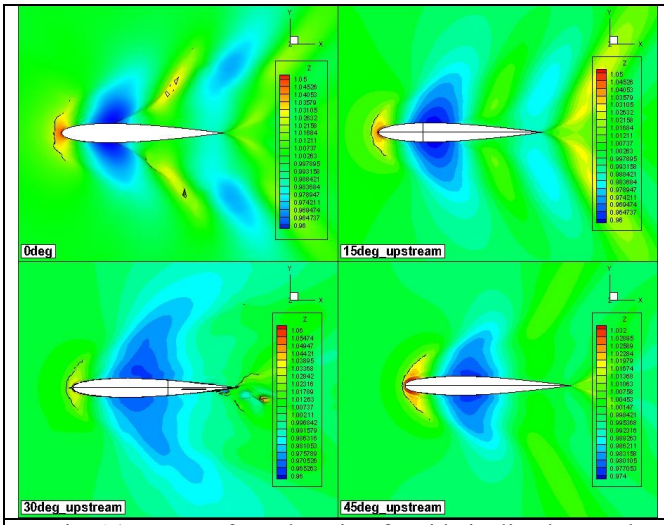

Fig. 14. Free surface elevation for side inclined toward upstream

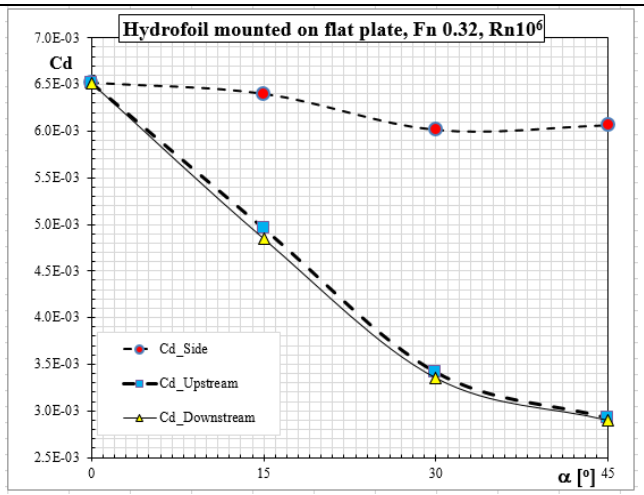

Fig. 15. Drag coefficient for the foil mounted on the flat plate, Fn=0.32, Rn=10^6.

Table 1. Drag coefficients of hydrofoil in respect to inclination angle, Fn=0.32, Rn= 10^6

Inclination direction	α [°]	Cdp	εdp [%Cdp (0°)]	Cdv	εdv [%Cdv (0°)]	Cd	εd [%Cd (0°)]
Side	0	0.00387	-	0.00652	-	0.00652	-
	15	0.00380	-1.87	0.00640	-1.80	0.00640	-1.80
	30	0.00343	-11.44	0.00601	-7.69	0.00601	-7.69
	45	0.00335	-13.57	0.00606	-6.94	0.00606	-6.94
Upstream	0	0.00387	-	0.00652	-	0.00652	-
	15	0.00229	-40.90	0.00496	-23.95	0.00496	-23.95
	30	0.00072	-81.28	0.00341	-47.64	0.00341	-47.64
	45	0.00022	-94.40	0.00292	-55.17	0.00292	-55.17
Downstream	0	0.00387	-	0.00652	-	0.00652	-
	15	0.00214	-44.67	0.00484	-25.65	0.00484	-25.65
	30	0.00074	-80.78	0.00335	-48.61	0.00335	-48.61
	45	0.00024	-93.69	0.00289	-55.58	0.00289	-55.58

4. CONCLUSIONS

In this study, a systematic numerical study of the flow around the junctions was presented and the influence of the inclination of the profile and the flow around the junction between a hydrofoil and a flat plate were studied. The results were presented for inclining the profile in 3 directions with three angle steps, 15, 30 and 45 degrees in respect to the upright profile, mounted on a flat plate. It was observed that from a hydrodynamic point of view the angle between hydrofoil and base plate to be less than 15 degrees in respect to the vertical direction of the hydrofoil so that horseshoe vortex to be reduced in intensity and the value of the hydrofoil drag to be minimal. Further studies are necessary with the hydrofoil mounted on a ship hull to validate the preliminary researches conclusions of the current study.

5. Acknowledgement

The research study presented in this article was developed in the frame of "Dunarea de Jos" University of Galati, Naval Architecture Research Centre.

REFERENCES

1. United Nations Framework Convention on Climate Change, (2008); Kyoto Protocol Reference Manual, available at: https://unfccc.int
2. International Maritime Organization, (2009), Second IMO GHG Study, Phase2, MEPC 59/INF.10, available at: https://www.imo.org/en/OurWork/Environment/Pages/Second-IMO-GHG-Study-2009.aspx
3. International Maritime Organization, (2011), MEPC 62nd session, 11-15 July, 2011, available at: https://www.imo.org/en/MediaCentre/SecretaryGeneral/Pages/MEPC-62.aspx
4. International Maritime Organization, (2021), MEPC 76th session, 10-17 June, 2021, available at: https://www.imo.org/en/MediaCentre/MeetingSummaries/Pages/MEPC76meetingsummary.aspx
5. Carlton J., (2007), *Marine Propellers and Propulsion*, *Elsevier*, 2nd edition, available at: https://ftp.idu.ac.id/wp-content/uploads/ebook/tdg/DESIGN%20SISTEM%20DAYA%20GERAK/Marine%20Propellers%20and%20Propulsion%20Second%20Edition.pdf
6. Çelik F. and Güner M. (2007). *Energy saving device of stator for marine propellers*, Ocean Engineering 34(5–6), 850-855;
7. Lungu A. and Ungureanu C. (2009). *Numerical simulation of the turbulent flow around a strut mounted on a plate* AIP Conference Proceedings 1168(1), 647-650.
8. Ungureanu C. Lungu A (2010). *Numerical Studies on Free Surface Flow around a Hydrofoil Mounted on a Plate* AIP Conference Proceedings 1281, 115-118.
9. Lungu A. (2021). *Energy-Saving Devices in Ship Propulsion: Effects of Nozzles Placed in Front of Propellers*, J. Mar. Sci. Eng., 9(2), 125.
10. *Wartsila Energoflow- Increase Energy Efficiency and Reduce Emissions* (2022), Wärtsilä Corporation Helsinky Finland available at: www.wartsila.com, accessed: 04/03/2022.
11. Mandru A. Pacuraru F. (2021). *The effect of appendages on ship resistance,* IOP Conf. Ser.: Mater. Sci. Eng., article number 1182 012041;
12. Yuchang Z. et al (2022). *Numerical investigations into the ventilation elimination mechanism of a surface-piercing hydrofoil,* Ocean Engineering, 243, article number 110225.

Received: June 02, 2022 / Accepted: December 15, 2022 / Paper available online: December 20, 2022

© International Journal of Modern Manufacturing Technologies